

# Chaos based on Riemannian geometric approach to Abelian-Higgs dynamical system

Tetsuji Kawabe\*

Physics Department, Department of Acoustic Design, Kyushu Institute of Design, Shiobaru, Fukuoka, 815-8540, Japan

(Received 18 June 2002; published 3 January 2003)

Based on the Riemannian geometric approach, we study chaos of the Abelian-Higgs dynamical system derived from a classical field equation consisting of a spatially homogeneous Abelian gauge field and Higgs field. Using the global indicator of chaos formulated by the sectional curvature of the ambient manifold, we show that this approach brings the same qualitative and quantitative information about order and chaos as has been provided by the Lyapunov exponents in the conventional and phenomenological approach. We confirm that the mechanism of chaos is a parametric instability of the system. By analyzing a close relation between the sectional curvature and the Gaussian curvature, we point out that the Toda-Brumer criterion becomes a sufficient condition to the criterion based on this geometric approach as to the stability condition.

DOI: 10.1103/PhysRevE.67.016201

PACS number(s): 05.45.-a, 11.15.Tk

There has long been an investigation in chaos of classical field theories such as the pure Yang-Mills theories [1], the Yang-Mills-Higgs (YMH) theories [2,3], and the Abelian gauge-Higgs (AH) theories [4] in order to understand general properties of their classical solutions. It has been shown that the classical solutions in the YMH and AH theories exhibit an order-to-chaos transition, i.e., a system has a threshold from order to chaos as the strength of the perturbation to the system increases. This phenomenon has been studied in the hope that it may provide additional knowledge about the vacuum structure of these field theories [5]. The chaos is detected by studying the instability of the system which is evolving with time after being perturbed initially. A quantitative characterization of chaos is mainly provided by the Lyapunov exponents of a given trajectory, which are the mean exponential rate of the divergence of trajectories surrounding it.

The stability or instability of the trajectory depends on the curvature of the manifold on which the trajectory is defined. In the conventional approach based on the abstract ergodic theory, the hyperbolicity of the manifold, i.e., the negative curvature manifold, provides an explanation of the origin of chaos [6]. Since the study of the stability of the system needs the information on the evolution of the perturbations of a given trajectory, the numerical simulation plays a central role and many numerical studies have been carried out by using algorithms under this conventional and phenomenological approach. The result of the numerical simulation, however, generally depends on the theory used for constructing the algorithms of computations. Many works so far have been done in almost the same theoretical framework based on the ergodic theory. Thus it must be important to study the dynamical models of the classical field theories from an approach different from the conventional one in order to examine the validity of the results on order and chaos obtained so far.

The purpose of this paper is to study the chaos of the spatially homogeneous model of the AH theory from a Riemannian geometric approach [7,8]. This approach is being

recently advocated to investigate the mechanism of the onset of chaos in the Hamiltonian systems and this has been applied to particular systems such as the Hénon-Heiles system [8] and the homogeneous YMH system [9]. Basic idea of this approach starts with a picture that the trajectories of a dynamical system can be viewed as geodesics on a Riemannian manifold endowed with a suitable metric. Based on this approach, the chaos stems from a parametric instability due to positive curvature fluctuations along the geodesics of the configuration space manifold. This mechanism is quite different from that based on the hyperbolicity in the conventional approach. Thus it is very interesting and important to study whether or not the Riemannian geometrical approach brings the results consistent with those on chaos of the AH dynamical system that have been provided by numerical studies in the conventional approach.

Let us begin with the Lagrangian density of the AH field theory given by [10]

$$L = -\frac{1}{4}F_{\mu\nu}F^{\mu\nu} + (D_\mu\phi)^*(D^\mu\phi) - V(\phi), \quad (1)$$

where the field strength  $F_{\mu\nu} = \partial_\mu A_\nu - \partial_\nu A_\mu$  and the covariant derivative  $D_\mu\phi = \partial_\mu\phi + iA_\mu\phi$ . The Higgs potential is  $V(\phi) = \kappa/4(|\phi|^2 - 1)^2$ . As we have rescaled both the electric charge and the symmetry-breaking scale to unity in the formulation, we have only the coupling constant  $\kappa$  as the remaining parameter. The spatially homogeneous approximation assumes that the field depends only on time  $t$  so that  $\partial_k A_k = 0$  and  $\partial_k\phi = 0$  hold in Eq. (1), where  $k=1,2,3$ . We assume  $A_k(t) = q_1(t)$  for all  $k$  components of the gauge field and  $\phi(t) = q_2(t)\exp(i\theta)$  for the Higgs field. Under this approximation in addition to the gauge condition of  $A_0 = 0$ , we obtain the nonlinear dynamical system described by the Hamiltonian as

$$H(\mathbf{p}, \mathbf{q}) = \frac{1}{2}(p_1^2 + p_2^2) + V(q_1, q_2), \quad (2)$$

$$V(\mathbf{q}) = \frac{1}{2}q_1^2q_2^2 + \frac{\kappa}{4}(q_2^2 - 1)^2, \quad (3)$$

\*Electronic address: kawabe@kyushu-id.ac.jp

where  $\mathbf{p}=(p_1, p_2)$ ,  $\mathbf{q}=(q_1, q_2)$ , and  $\mathbf{p}=\dot{\mathbf{q}}$ . In the Riemannian geometric approach [8], the sectional curvature  $K^{(2)}$ , defined as

$$K^{(2)}(\mathbf{p}, \mathbf{q}) = \frac{1}{2(E-V)} \left[ \frac{\partial^2 V}{\partial q_1^2} p_2^2 + \frac{\partial^2 V}{\partial q_2^2} p_1^2 - 2 \frac{\partial^2 V}{\partial q_1 \partial q_2} p_1 p_2 \right], \quad (4)$$

plays a central role to study the dynamical behavior of a system with two degrees of freedom. This  $K^{(2)}$  controls the stability of the Jacobi-Levi-Civita (JLC) equation for geodesic spread. Since the instability of the system stems from the condition of  $K^{(2)} < 0$ , the global indicator of the order-to-chaos transition is the integral  $\langle K_{(-)}^{(2)} \rangle$  of the negative values assumed by  $K^{(2)}$  over a constant energy surface  $\Sigma_E$ , which is defined by

$$\langle K_{(-)}^{(2)} \rangle = \frac{1}{A(\Sigma_E)} \int_{\Sigma_E} d\sigma_E K^{(2)} = \frac{1}{A(\Sigma_E)} \int d\mathbf{p} d\mathbf{q} \delta[H(\mathbf{p}, \mathbf{q}) - E] \Theta(-K^{(2)}) K^{(2)}(\mathbf{p}, \mathbf{q}), \quad (5)$$

where  $\Theta$  is the step function, i.e.,  $\Theta(x) = 0$  for  $x < 0$  while  $\Theta(x) = 1$  for  $x \geq 0$ . The area  $A(\Sigma_E)$  in Eq. (5) is given by

$$A(\Sigma_E) = \int_{\Sigma_E} d\sigma_E = \int d\mathbf{p} d\mathbf{q} \delta[H(\mathbf{p}, \mathbf{q}) - E]. \quad (6)$$

It should be noted that this quantity  $\langle K_{(-)}^{(2)} \rangle$  depends only on the geometric property of the ambient manifold, and it does not require any numerical integration of the equations of motion involved in the dynamics.

Let us first study this global indicator  $\langle K_{(-)}^{(2)} \rangle$ . The sectional curvature  $K^{(2)}$  corresponding to the AH dynamical system of Eqs. (2) and (3) is given by

$$K^{(2)}(\mathbf{p}, \mathbf{q}) = \frac{1}{p_1^2 + p_2^2} [q_2^2 p_2^2 + (q_1^2 + 3\kappa q_2^2 - \kappa) p_1^2 - 4q_1 q_2 p_1 p_2]. \quad (7)$$

The Hamiltonian (2) describes the motion of a particle in a two-dimensional potential well  $V(q_1, q_2)$ . The potential contour defined by  $V=E$  is determined once the coupling constant  $\kappa$  is given. We introduce the parameter  $Q \equiv 4E/\kappa$  to characterize the potential contour. The contour is closed when  $Q \leq 1$ , while the contour is open to the  $q_1$ -axis direction when  $Q > 1$ . The contour of the potential for  $0.05 \leq Q \leq 1.0$  in  $q_2 > 0$  region is shown for the case of  $\kappa = 1.0$  in Fig. 1. Thus the system is completely described by  $Q$  and  $\kappa$  and the calculation of  $\langle K_{(-)}^{(2)} \rangle$  has to be done under the condition of  $Q \leq 1$  to confine the trajectories in a finite region. We have calculated  $\langle K_{(-)}^{(2)} \rangle$  for the range  $Q = 0.05 \sim 1.0$  while varying the energy  $E$  and the coupling constant  $\kappa$ . Figure 2 shows the result of  $\langle K_{(-)}^{(2)} \rangle$  versus  $Q$  obtained from the computation at different values of  $\kappa = 0.1, 0.5, 1.0, 5.0$ , and  $10.0$ . The integral  $\langle K_{(-)}^{(2)} \rangle$  is zero for small  $Q < 0.4$  and begins to increase for

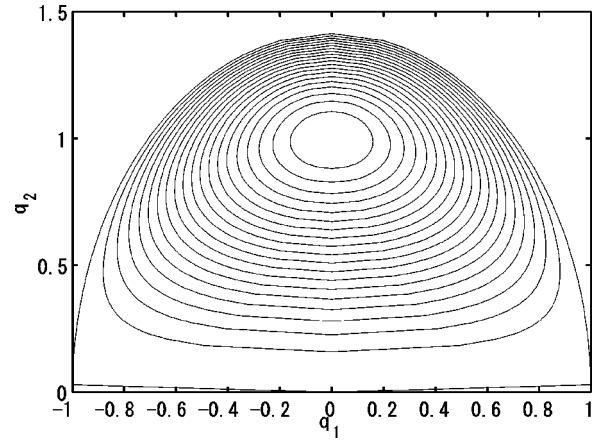


FIG. 1. Potential level contours for  $0.05 \leq Q \leq 1.0$  at  $\kappa = 1.0$ . The innermost contour corresponds to  $Q = 0.05$  while the outermost one corresponds to  $Q = 1.0$ .

larger  $Q$  irrespective of the values of  $\kappa$ . The transition from order to chaos seems to occur at almost the same value of  $Q = 0.40 \sim 0.50$ .

Second we try to study whether or not the global structure determined by  $\langle K_{(-)}^{(2)} \rangle$  is consistent with the result obtained by the conventional approach. The integral  $\langle K_{(-)}^{(2)} \rangle$  is essentially related to the ratio  $\mu$  between the area covered by the regular trajectories and the total area in the phase space accessible to the motions. The ratio  $\mu$  is quantitatively determined by calculating the Lyapunov exponent of the system, which is frequently used as a reliable indicator of chaos in the conventional and phenomenological approach. The Lyapunov exponent  $\lambda$  gives the average rate of the exponentially fast divergence or convergence of two nearby trajectories in the phase space. A chaotic system corresponds to  $\lambda > 0$ , while a regular one corresponds to  $\lambda = 0$ . Numerical determination of the ratio  $\mu$  is done by using the fraction of initial points leading to regular state,  $\lambda = 0$ . This method has some practical difficulties because the condition for a regular state,  $\lambda = 0$ , is not numerically realized in finite integration

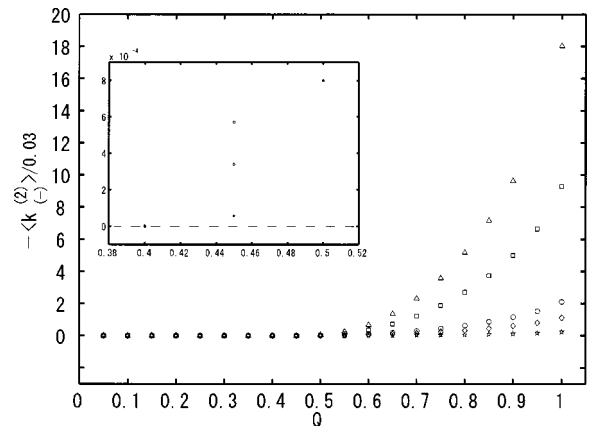


FIG. 2. Plots of  $-\langle K_{(-)}^{(2)} \rangle / 0.03$  vs  $Q$  for the AH dynamical system. The correspondence of a marker to a value of  $\kappa$  is as follows: the triangle is  $\kappa = 10.0$ , the square is  $\kappa = 5.0$ , the circle is  $\kappa = 1.0$ , the diamond is  $\kappa = 0.5$ , and the star is  $\kappa = 0.1$ .

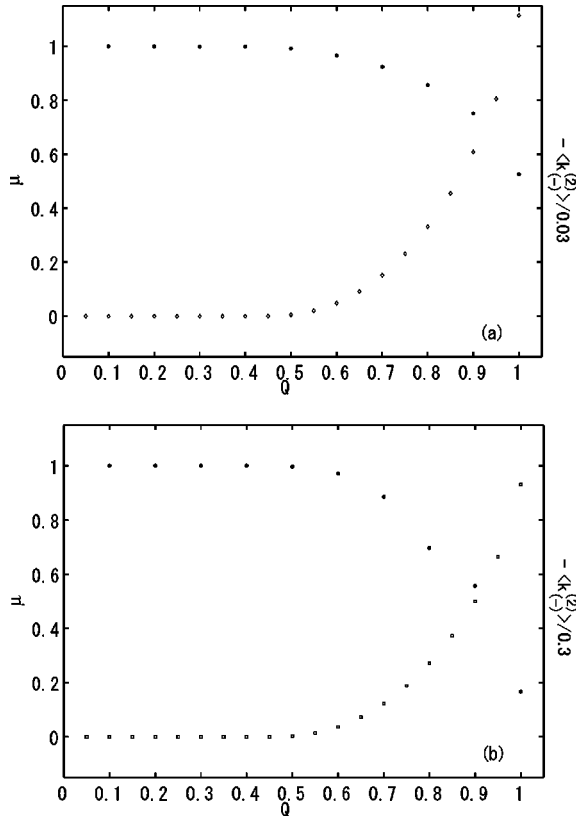


FIG. 3. Plots of  $\mu$  (full dots) vs  $Q$  at different values of  $\kappa$  for the AH dynamical system: (a)  $\kappa=0.5$  and (b)  $\kappa=5.0$ . In order to compare with  $\mu$ , the global indicator  $\langle K_{(-)}^{(2)} \rangle$  is also plotted with a suitable scale factor.

time. Thus we need to assume that the value of  $\lambda$  is zero whenever it becomes less than  $\lambda_c$ , a certain value of  $\lambda$  after sufficiently time evolution of the system. We took  $\lambda_c = 0.001$  because we confirmed from many simulations that all values of  $\lambda < \lambda_c$  approach zero. For each value of  $Q = 0.05 \sim 1.0$  we have computed the Lyapunov exponents  $\lambda$  for 5000 random initial points. For each initial point we made the  $10^8$  successive iterations. The calculation of the ratio  $\mu$  was done for several values of  $\kappa$ . Figures 3(a) and 3(b) show the result of  $\mu$  (full dots) versus  $Q$  for the case of  $\kappa=0.5$  and  $\kappa=5.0$ , respectively. The ratio  $\mu$  exhibits almost the same tendency in Figs. 3(a) and 3(b):  $\mu$  stays 1.0 for small  $Q < 0.4$ , where the whole area in the phase space is covered by regular trajectories. On the other hand,  $\mu$  begins to decrease below 1.0 for larger  $Q$ , where the measure of chaotic trajectories begins to increase. In Figs. 3(a) and 3(b) we also put  $\langle K_{(-)}^{(2)} \rangle$  of Fig. 2 with a suitable scale factor for graphical reasons to compare with  $\mu$ . We see that  $\langle K_{(-)}^{(2)} \rangle$  starts increasing at the same value of  $Q$  at which  $\mu$  begins to decrease. Therefore we can confirm that  $\langle K_{(-)}^{(2)} \rangle$  brings the same qualitative and quantitative information that is provided by the Lyapunov exponents in the conventional approach. For the numerical integration for the equations of motion, we used a fourth-order Runge-Kutta routine with a time step,  $\Delta t$ , equal to  $10^{-2}$ . We chose the size of  $\Delta t$  so that any reduction of the size does not cause significant change in the results.

Third we study the mechanism of the instability of this system. In the Riemannian geometric approach, the instability is determined by the way that the separation between nearby geodesics evolves with time. The evolution of such a geodesic spread is described by the JLC equation. This JLC equation can be written in the form of the Hill equation as [8]

$$\frac{d^2 Y(t)}{dt^2} + \Omega(t)Y(t) = 0, \quad (8)$$

where

$$\Omega(t) = \left[ \Delta V + \frac{3(\nabla V)^2}{2W} \right] - \frac{3}{4W^2} \left[ p_1 \frac{\partial V}{\partial q_1} + p_2 \frac{\partial V}{\partial q_2} \right]^2 - \frac{1}{2W} \sum_{i,k} \frac{\partial^2 V}{\partial q_i \partial q_k} p_i p_k. \quad (9)$$

Here  $\Delta V = \partial^2 V / \partial q_1^2 + \partial^2 V / \partial q_2^2$  is the Euclidean Laplacian and  $\nabla V = (\partial V / \partial q_1, \partial V / \partial q_2)$  is the Euclidean gradient, and  $W = E - V(q_1, q_2)$ . The quantity  $Y(t)$  gives a measure of the geodesic spread. This Hill equation determines the stability of system. The unstable solutions appear when Eq. (8) satisfies the condition of  $\Omega(t) < 0$ . However, this condition is not the only way to make unstable solutions. From the viewpoint of the nonlinear oscillation [11] we have another chance to get unstable solutions through a parametric resonance. The instability due to the parametric resonance is expected to occur when the parameters characterizing the system vary periodically in time. In this case the stable solution becomes unstable even if the system satisfies the condition of  $\Omega(t) > 0$  for each value of the parameters. Since this geometric approach claims that the parametric resonance is a main mechanism of instability, it is important to investigate whether or not such a phenomenon indeed occurs. We have calculated both  $Y(t)$  and  $\Omega(t)$  for various initial values at low  $Q$  (ordered system) and at high  $Q$  (chaotic system). Figure 4(a) shows the absolute value of the envelope  $|Y(t)|$  for  $Q=0.05$  at  $\kappa=5.0$ , where  $|Y(t)|$  presents a weak exponential growth at an early stage of time evolution but becomes a constant in longer times. Since the regular motion is characterized by a bounded or a linearly growing oscillation, this behavior of Fig. 4(a) is reasonable. Figure 4(b) shows the frequency  $\Omega(t)$  for the same values of  $Q$  and  $\kappa$  as those in Fig. 4(a), where  $\Omega(t)$  is positive as expected. On the other hand, Figs. 4(c) and 4(d) present the results for  $Q=1.0$  at  $\kappa=5.0$ , where the envelope  $|Y(t)|$  is exponentially growing while the frequency  $\Omega(t)$  stays always positive. The behavior of the envelope  $|Y(t)|$  in Fig. 4(c) is consistent with the behavior of nearby trajectories used for the calculation of the Lyapunov exponents. Thus we can confirm that the onset of chaos in this Riemannian geometric approach is due to the parametric instability of the system which always satisfies the condition of  $\Omega(t) > 0$  as shown in Fig. 4(d).

Fourth we consider the criterion on the stability of the system. The stability connects with the curvature of the manifold. In the geometric Riemannian approach the sign of

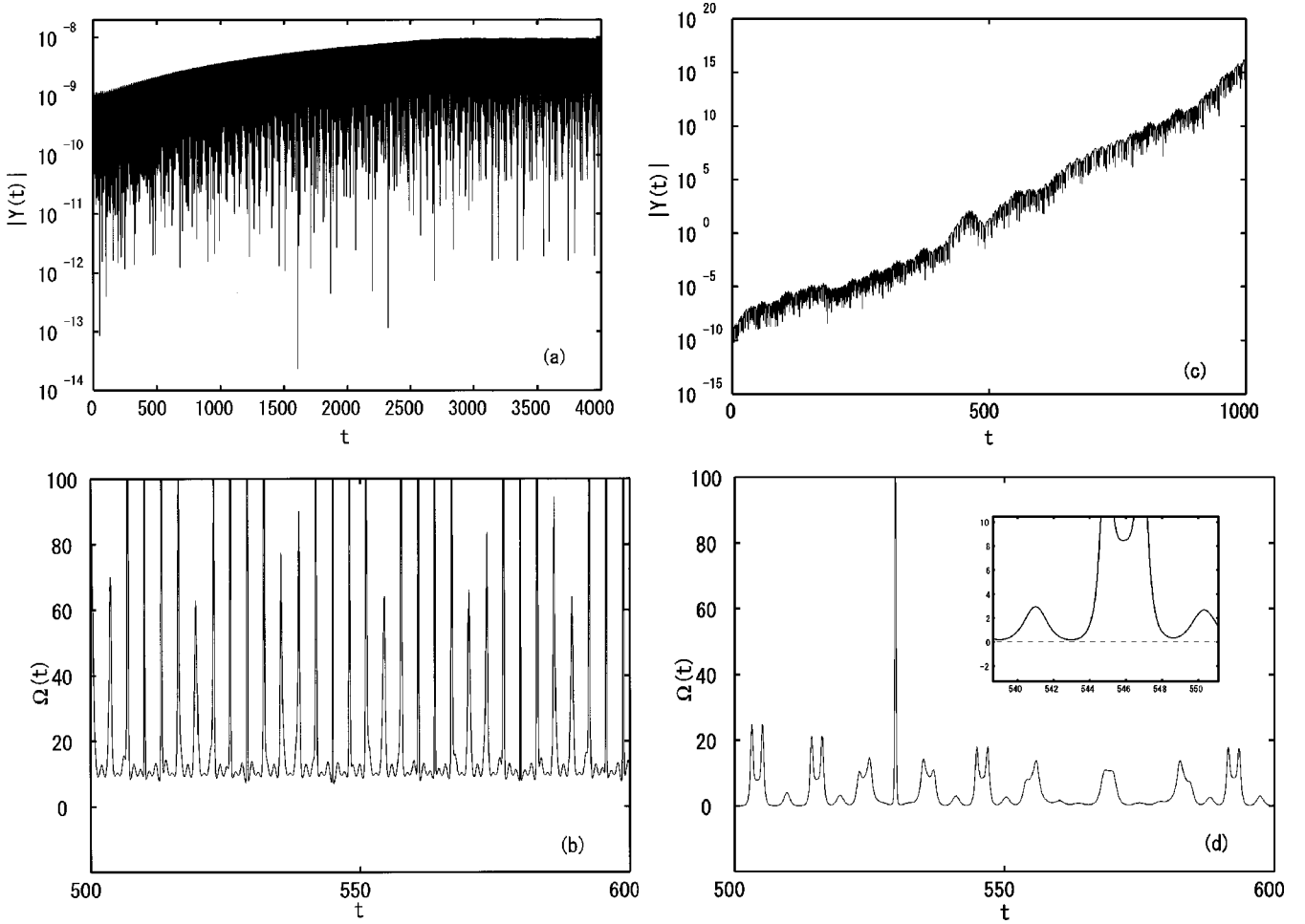


FIG. 4. Plots of the envelope  $|Y|$  and the frequency  $\Omega$  vs time for the AH dynamical system with  $\kappa=5.0$ : (a)  $|Y|$  and (b)  $\Omega$  for an initial value at  $Q=0.05$  (ordered system), while (c)  $|Y|$  and (d)  $\Omega$  for an initial value at  $Q=1.0$  (chaotic system).

the sectional curvature  $K^{(2)}$  of Eq. (4) determines the stability of the system: i.e., a stable state is realized if  $K^{(2)}>0$  while the instability occurs if  $K^{(2)}<0$ . On the other hand, the stability of the system can be also determined by using the Gaussian curvature defined by

$$G(\mathbf{q}) = \frac{\partial^2 V}{\partial q_1^2} \frac{\partial^2 V}{\partial q_2^2} - \left( \frac{\partial^2 V}{\partial q_1 \partial q_2} \right)^2. \quad (10)$$

This quantity is equivalent to the product of the eigenvalues characterizing the two-dimensional flow in the tangent dynamics equation for the perturbed trajectories and the sign of  $G$  controls the time evolution of trajectories. If we have a region where  $G$  is negative, so is one of the eigenvalues, and for this negative eigenvalue the perturbed trajectory evolves exponentially with time. In this case the system exhibits an exponential instability in this region, such as the C system [6]. In order to see the possible relation between  $G$  and  $K^{(2)}$ , we have calculated them for various initial values leading to regular trajectories or chaotic ones. Figure 5 gives examples of the time evolution of  $G$  and  $K^{(2)}$ . For the regular trajectories both  $G$  and  $K^{(2)}$  always have positive values, as expected, as shown in Fig. 5(a), while for chaotic ones they

seem not to have any relation with each other at first glance at Fig. 5(b). However, from more careful observation of Fig. 5(b) we find the fact that  $K^{(2)}$  becomes always positive when  $G$  is positive.

This observation can be supported as follows: In the AH dynamical system the stability matrix defined by  $m_{ij} = \partial^2 V / \partial q_i \partial q_j$  becomes  $m_{11} = q_2^2$ ,  $m_{22} = q_1^2 + 3\kappa q_2^2 - \kappa$ , and  $m_{12} = m_{21} = 2q_1 q_2$ . Let us put  $m_{ij}$  as  $\alpha = m_{11}$ ,  $\beta = m_{22}$ , and  $\gamma = m_{12}$ . Since the potential  $V(q_1, q_2)$  is symmetric under  $q_1 \rightarrow -q_1$  and  $q_2 \rightarrow -q_2$ , the phase space we should consider is confined to the first quadrant so that  $\gamma > 0$  holds. If  $\beta > 0$ , the sectional curvature  $K^{(2)}$  of Eq. (7) can be written as

$$2WK^{(2)} = \alpha p_2^2 + \beta p_1^2 - 2\gamma p_1 p_2 = (\sqrt{\alpha} p_2 - \sqrt{\beta} p_1)^2 + 2(\sqrt{\alpha\beta} - \gamma) p_1 p_2. \quad (11)$$

If  $p_1 p_2 < 0$ , it is obvious from the second part of Eq. (11) that  $K^{(2)} > 0$ , i.e., the system is stable. If  $p_1 p_2 > 0$ , it is found from the third part of Eq. (11) that  $K^{(2)} > 0$  holds as long as the condition  $\sqrt{\alpha\beta} - \gamma > 0$  holds. This condition implies that the

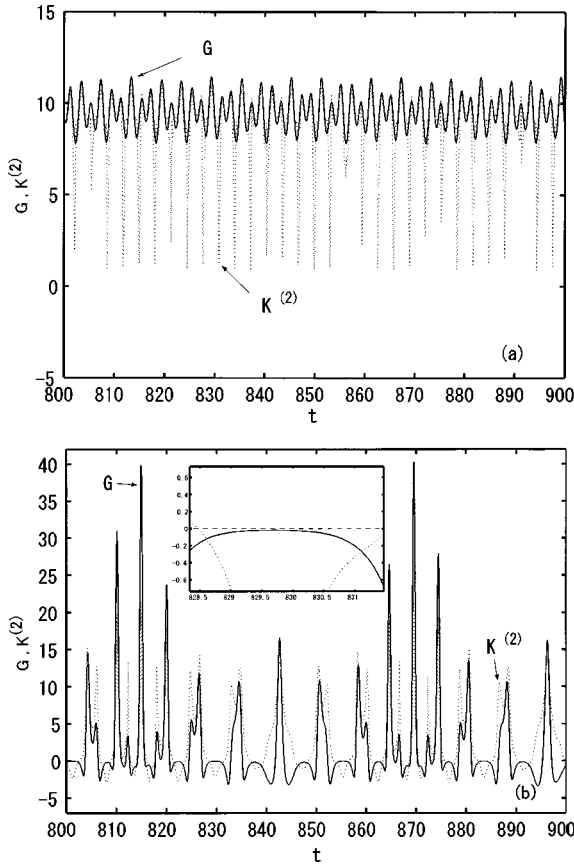


FIG. 5. Plots of  $G$  (solid line) and  $K^{(2)}$  (dotted line) vs time for the AH dynamical system with  $\kappa=5.0$ : (a)  $G$  and  $K^{(2)}$  for an initial value at  $Q=0.05$  (ordered system), while (b)  $G$  and  $K^{(2)}$  for an initial value at  $Q=1.0$  (chaotic system).

Gaussian curvature  $G$  is positive because of  $G=(\sqrt{\alpha\beta} + \gamma)(\sqrt{\alpha\beta} - \gamma)$ . This means that the stable condition  $G>0$  is a sufficient condition for  $K^{(2)}>0$ , i.e.,  $G>0 \Rightarrow K^{(2)}>0$ . The contraposition also holds, i.e.,  $K^{(2)}<0 \Rightarrow G<0$ , which strictly holds as shown in the inset in Fig. 5(b). This Gaussian curvature has a direct connection with the Toda-Brumer criterion [12] for studying the stability of the dynamical system. The present analysis reveals that the Toda-Brumer criterion is a sufficient condition to the criterion based on the sectional curvature as to the stability condition.

Finally let us consider the meaning of the condition  $\beta > 0$ . Since this condition gives the inequality as  $q_1^2 + 3\kappa q_2^2 > \kappa$ , the allowed region in the  $(q_1, q_2)$  plane is the outside of the ellipse, whose major and minor axes are given by  $(q_1, q_2) = (-\sqrt{\kappa}, 0), (\sqrt{\kappa}, 0), (0, -1/\sqrt{3}),$  and  $(0, 1/\sqrt{3})$ . On the other hand, from the equation  $V(0, q_2) = E$  on the potential contour, we see that the physically allowed values of  $q_2$  are confined to the region as  $\sqrt{1 - \sqrt{Q}} \leq q_2 \leq \sqrt{1 + \sqrt{Q}}$  for  $0 \leq Q \leq 1$ . The above inequality implies the relation that  $1/\sqrt{3} < (1 - \sqrt{Q})^{1/2}$ , i.e.,  $Q < \frac{4}{9} = 0.444 \dots \equiv Q^*$ . Thus we find that the system becomes stable when  $Q < Q^*$  so that  $Q^*$  will be regarded as the threshold value of the transition from order to chaos. It should be noticed that this threshold value  $Q^*$  seems to be consistent with the value observed in Fig. 2, which distinguishes between  $\langle K_{(-)}^{(2)} \rangle = 0$  and  $\langle K_{(-)}^{(2)} \rangle \neq 0$ .

In conclusion, we have studied the dynamical properties of the AH dynamical system from the Riemannian geometric approach. From the analyses on the global indicator  $\langle K_{(-)}^{(2)} \rangle$  we have found that this system shows the transition from order to chaos for a wide range of  $\kappa$  and  $E$  satisfying  $Q \leq 1$ . The behavior of  $\langle K_{(-)}^{(2)} \rangle$  is completely consistent with the behavior of the ratio  $\mu$  determined by the Lyapunov exponents that have been used in the conventional approach. Especially the threshold value  $Q^*$  for the order-to-chaos transition is almost the same in both approaches. Through a detailed quantitative comparison between the Riemannian geometric analysis and the traditional one we have confirmed that the order-to-chaos transition is an inherent characteristics of the AH dynamical system.

The above conclusion is based on the result that the quantity  $\langle K_{(-)}^{(2)} \rangle$  obtained by computing the microcanonical average of the sectional curvature  $K^{(2)}$  agrees with the ratio  $\mu$  determined by using the values of the Lyapunov exponent  $\lambda$  for many initial conditions. This ratio is the fraction of the numbers of initial conditions for which  $\lambda = 0$  and  $\lambda > 0$ . Although the numerical calculation of  $\lambda$  has been done for a very large number of initial conditions, the amount of numerical calculation is not enough to obtain the ensemble average from which  $\mu$  can be determined. Nevertheless, in the present analyses we have found that  $\mu$  agrees with  $\langle K_{(-)}^{(2)} \rangle$ . Thus we might claim that the ergodicity is not required when we estimate the relative weight of stable versus unstable trajectories such as  $\mu$ . Since the present analysis is restricted to the specific model of the AH theory, it is a very important issue to study whether or not this claim is generally valid in many dynamical systems.

We have also found the relation of the stochasticity criterion between  $\langle K_{(-)}^{(2)} \rangle$  and the Gaussian curvature  $G$ , with the aid of a concrete calculation of  $K^{(2)}$  in Eq. (7) and  $G$  in Eq. (10). Since the Gaussian curvature  $G$  provides the basis of the Toda-Brumer criterion, it will be an interesting issue to derive a mathematical relation between  $G$  and  $K^{(2)}$  more directly from the definition of the Riemannian curvature tensor, the Ricci curvature, and the Gaussian curvature and then to clarify a close link between the curvature of the manifold and the stability of the trajectories.

The present work gives one concrete example showing that the Riemannian geometric approach is very effective for research on chaos in the Hamiltonian dynamical systems with two degrees of freedom, where the dominant mechanism of chaos is due to the parametric instability. It will be a very important issue to apply this approach to the high-dimensional case [3] such as the YMH field theory with space-time dependence whose magnetic monopole solution has been shown to exhibit the order-to-chaos transition in the conventional and phenomenological analyses.

#### ACKNOWLEDGMENTS

I would like to thank H. Fujisaka, T. Hada, and S. Ohta for many helpful discussions.

- [1] S.G. Matinyan, E.B. Prokhorenko, and G.K. Savvidy, Pis'ma Zh. Éksp. Teor. Fiz. **44**, 109 (1986) [JETP Lett. **44**, 138 (1986)]; Nucl. Phys. B **298**, 414 (1988); T. Kawabe and S. Ohta, Phys. Rev. D **41**, 1983 (1990).
- [2] S.G. Matinyan, E.B. Prokhorenko, and G.K. Savvidy, Yad. Fiz. **50**, 284 (1989) [Sov. J. Nucl. Phys. **50**, 178 (1989)]; M.P. Joy and M. Sabir, J. Phys. A **25**, 3721 (1992); C.N. Kumar and A. Khare, *ibid.* **22**, L849 (1989); B.A. Bambah, S. Lakshimbala, C. Mukku, and M.S. Sriram, Phys. Rev. D **47**, 4677 (1993); J. Segar and M.S. Sriram, *ibid.* **53**, 3976 (1996); D. Ebert, V.Ch. Zhukovsky, and M.V. Rogal, *ibid.* **65**, 065017 (2002).
- [3] T. Kawabe and S. Ohta, Phys. Rev. D **44**, 1274 (1991); T. Kawabe, Phys. Lett. B **274**, 399 (1992); T. Kawabe, J. Phys. A **26**, L1131 (1993); T. Kawabe and S. Ohta, Phys. Lett. B **334**, 127 (1994).
- [4] T. Kawabe, Phys. Lett. B **343**, 254 (1995); T. Kawabe and S. Ohta, *ibid.* **392**, 433 (1997); S. Ohta and T. Kawabe, Phys. Rev. D **56**, 3660 (1997); T. Kawabe and S. Ohta, *ibid.* **61**, 105013 (2000).
- [5] T.S. Biro, S.G. Matinyan, and B. Mueller, *Chaos and Gauge Field Theory*, Lecture Notes in Physics Vol. 56 (World Scientific, Singapore, 1994).
- [6] A.J. Lichtenberg and M.A. Lieberman, *Regular and Chaotic Dynamics* (Springer, Berlin, 1992).
- [7] M. Pettini, Phys. Rev. E **47**, 828 (1993); L. Casetti and M. Pettini, *ibid.* **48**, 4320 (1993); L. Casetti, R. Livi, and M. Pettini, Phys. Rev. Lett. **74**, 375 (1995); L. Casetti, M. Pettini, and E.G.D. Cohen, Phys. Rep. **337**, 237 (2000).
- [8] M. Cerruti-Sola and M. Pettini, Phys. Rev. E **53**, 179 (1996).
- [9] K. Ramasubramanian and M.S. Sriram, Phys. Rev. E **64**, 046207 (2001).
- [10] H.B. Nielsen and P. Olesen, Nucl. Phys. B **61**, 45 (1973).
- [11] R.Z. Sagdeev, D.A. Usikov, and G.M. Zaslavsky, *Nonlinear Physics* (Harwood Academic, London, 1988).
- [12] M. Toda, Phys. Lett. **48A**, 335 (1974); P. Brumer and W. Duff, J. Chem. Phys. **65**, 3566 (1976).